J Appl Electrochem (2013) 43:399–405
DOI 10.1007/s10800-013-0525-6

ORIGINAL PAPER

Field emission properties of Cu/multiwalled carbon nanotube composite films fabricated by an electrodeposition technique

Susumu Arai · Eri Shinada · Takashi Saito

Received: 19 September 2012 / Accepted: 9 January 2013 / Published online: 19 January 2013

Abstract Composite films of Cu and multiwalled carbon nanotubes (MWCNTs) were fabricated by an electrodeposition technique, and their field emission properties were examined. Commercially available MWCNTs with various diameters (60–150 nm) were used. The microstructure of the composite films was analyzed by scanning electron microscopy and the field emission properties were measured using a diode-type system. Cu/MWCNT composite films with homogeneous dispersion of MWCNTs were fabricated using each type of MWCNT. Bare MWCNTs were present on the surface of the composite films and the ends of the protruding tips were fixed by the deposited copper matrix. The composite films produced clear emission currents and the corresponding Fowler–Nordheim (F–N) plots showed that these were field emission currents. The turn-on electric field tended to decrease with decreasing MWCNT diameter. A light-emitting device incorporating the Cu/MWCNT composite film as a field emitter was fabricated, and its light-emitting properties were investigated. Light emission with a brightness of around 100 cd m^{-2} was observed for approximately 100 h.

Keywords Cu · Carbon nanotube · Composite · Electrodeposition · Field emission

1 Introduction

Carbon nanotubes (CNTs) [1, 2] possess excellent mechanical characteristics, such as high tensile strength and high elastic modulus, as well as high thermal conductivity. Research efforts on composite materials with CNTs as fillers for forming high strength materials [3–7] and high thermal conductivity materials [8, 9] have thus been continually increasing. Furthermore, CNTs have high aspect ratios, high chemical inertness, and good electrical conductivity, and accordingly are potential field emission electron sources [10, 11]. Field emitters using CNTs have been fabricated by various methods. The direct growth method [12–14] shows good control of the alignment, density, diameter, and length of CNTs, but is limited by the scalability of the substrate size and the growth temperature. The screen printing method [15–19] has good scalability, but outgassing from the organic vehicle in the paste degrades the CNTs. The spray deposition method [20] has good scalability, but yields poor adhesion. Thus, each of these methods has drawbacks for practical use.

Recently, the field emission properties of metal/CNT composite films formed by a chemical displacement plating method [21] and an electroless composite plating method [22] were reported. We have been investigating metal/CNT composite plating techniques and we previously reported patterned Cu/multiwalled carbon nanotube (MWCNT) composite field emitters formed by an electrodeposition technique [23]; we also elucidated the effects of varying the plating bath composition on the field emission properties of the Cu/MWCNT composite plating films [24]. This metal/CNT composite film emitter is expected to have several advantages. First, the CNTs are fixed by a metal matrix, resulting in good adhesion. Second, there are no organic substances and thus there is no degradation of the CNTs. Moreover, the electroplating method has good scalability and is of low cost. However, in this previous work, we used large, 150-nm-diameter MWCNTs.

In the present study, we fabricated Cu/MWCNT composite plating films using MWCNTs of various diameters and evaluated their field emission properties.

S. Arai (✉) · E. Shinada · T. Saito
Department of Chemistry and Material Engineering,
Faculty of Engineering, Shinshu University, 4-17-1 Wakasato,
Nagano-shi, Nagano 380-8553, Japan
e-mail: araisun@shinshu-u.ac.jp

2 Experimental

2.1 Chemicals

Three kinds of MWCNTs with different diameters were used in the present study. These are commercially available CNTs, including VGCF and VGCF-S (Showa Denko Co. Ltd.) which have diameters of 150 and 80 nm, respectively, and MWNT-7 (Mitsui & Co., Ltd.) which has a diameter of 60 nm. All the MWCNTs were approximately 15 μm in length. $CuSO_4 \cdot 5H_2O$ and H_2SO_4 (Wako Pure Chemical Industries, Ltd.) used in the study were special grade materials. Polyacrylic acid, with a mean molecular weight of 5,000, (PA5000: Wako Pure Chemical Industries, Ltd.) was used and was first grade. Pure water from an electrodialysis water purifier (RFP343RA, ADVANTEC MFS, Inc.) was used in all the experiments.

2.2 Fabrication of Cu/MWCNT composite films

A sulfuric copper plating bath (0.85 M $CuSO_4 \cdot 5H_2O$ + 0.55 M H_2SO_4) was used as the base plating bath. The MWCNTs are hydrophobic and consequently did not disperse uniformly in the base bath. Homogeneous dispersion of the MWCNTs was achieved by the addition of polyacrylic acid to the base bath with stirring. The compositions of the composite plating baths were 0.85 M $CuSO_4 \cdot 5H_2O$ + 0.55 M H_2SO_4 + 2.0×10^{-5} M PA5000 + x g dm^{-3} MWCNTs. Electrodeposition was performed at 25 °C with agitation by bubbling air under the galvanostatic condition of 1 A dm^{-2}. A commercially available electrolytic cell (Model I, Yamamoto-Ms Co., Ltd.) with internal dimensions of 65 × 65 × 95 mm^3 was employed for the electrodeposition. The volume of the plating bath was 250 cm^3. A pure Cu plate (JIS C1201P) with an exposed surface area of 10 cm^2 (3 × 3.33 cm) was used as the cathode. A copper plate containing a small amount of phosphorus (A-53-M1-P08-08, Yamamoto-Ms Co., Ltd.) was used as the anode.

2.3 Microstructure of Cu/MWCNT composite films

The surface and cross-sectional morphologies of the composite films were examined by field emission scanning electron microscopy (FE-SEM; JSM-7000F, JEOL Ltd.) using an acceleration voltage of 5 kV. Exclusive sample preparation equipment (cross-section polisher, SM-09010 JEOL Ltd.) was used to prepare cross-sectional samples for the FE-SEM observations.

2.4 Field emission properties of Cu/MWCNT composite films

Field emission properties were measured using a diode-type field emission measurement system (CN-EMS30, ULVAC Inc.). The base pressure of the field emission chamber was around 10^{-5} Pa. The dimensions of the composite film cathodes were 3 × 3.3 cm. A cylindrical stainless steel electrode with a 0.785 cm^2 facing surface area was used as the anode. The gap between the anode and the composite film surface was 1 mm. The emission current density was calculated by dividing the measured emission current by the anode facing surface area (0.785 cm^2).

2.5 Light emission properties

A light-emitting device incorporating the Cu/MWCNT composite film emitter cathode developed in this work was fabricated. The light emitting device is a vacuum tube-type device with a triode configuration. The vacuum tube was made of borosilicate glass. The dimensions of the Cu/MWCNT composite film cathode were 2 × 2 cm. A mesh stainless steel plate (hole size: 0.5 × 0.5 mm, interval: 0.1 mm) was used as the gate. ITO-coated glass spread with a white type phosphor over a 2 cm^2 area was used as the anode. The white-type phosphor consisted of typical red, green, and blue phosphors (red: P22-RE3, green: P22-GN4, blue: LP-B1. Kasei Optonix, Ltd.). The gap between the cathode and the gate was 1 mm and the gap between the gate and the anode was 3 mm. Thus, the gap between the cathode and the anode was 4 mm. The pressure inside the device was 5×10^{-5} Pa. DC power was applied to each electrode and the brightness of the light-emitting device was measured using a luminance meter (CS-200, Konica-Minolta Holdings, Inc.) in a dark environment created using a black curtain.

3 Results and discussion

Figure 1 shows surface SEM images of the Cu/VGCF composite films electrodeposited using plating baths with different concentrations of VGCFs. The VGCFs are present on the surface of the composite films. The number of VGCFs increased with increasing VGCF concentration (0.1–2 g dm^{-3}) in the plating baths. The orientations of the VGCFs seemed to be random. VGCFs on the film surface were present without aggregation with VGCF concentrations ranging from 0.1 to 1 g dm^{-3} (Fig. 1a). For a VGCF concentration of 2 g dm^{-3}, aggregates of VGCFs are seen (Fig. 1b). For a VGCF concentration >2 g dm^{-3}, the number of VGCFs on the film surface decreased. It is to be noted that the VGCFs were not coated with copper, in other words, bare VGCFs were present on the surface of the composite films. It is known that MWCNTs show electrical conductivity in the axial direction [25]. Therefore, when an MWCNT is incorporated into a deposited metal matrix, the

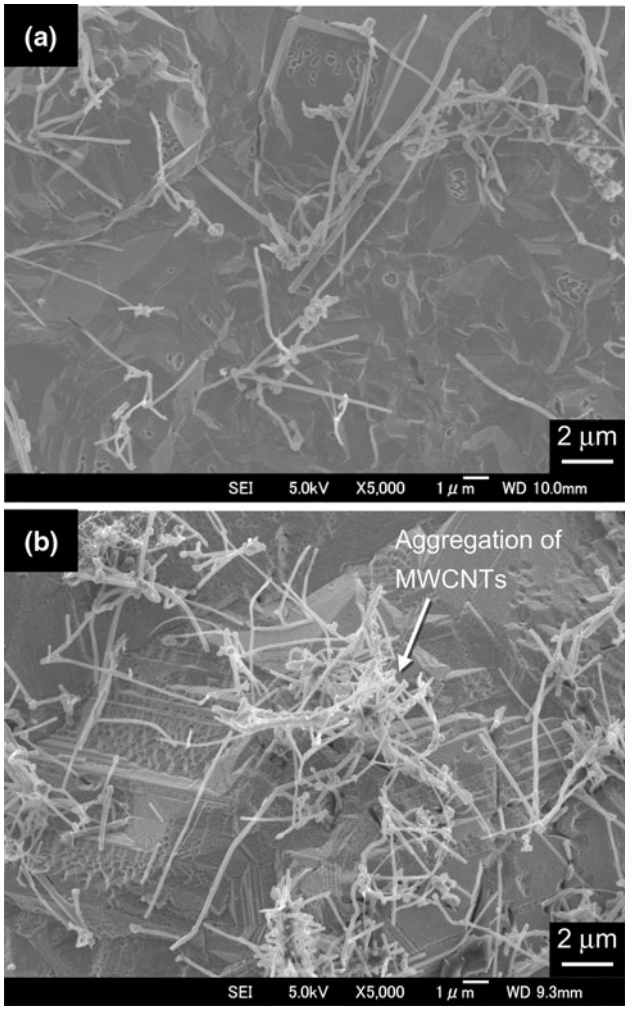

Fig. 1 Surface SEM images of Cu/VGCF composite films. The VGCF concentration in the plating baths was **a** 0.5 g dm^{-3} and **b** 2 g dm^{-3}

metal may additionally electrodeposit on the protruding ends of the incorporated MWCNTs [26, 27]. We have already reported the electrodeposition behavior of copper for Cu/MWCNT composite films [28]. Copper can electrodeposit not only on the deposited copper matrix but also on the protruding ends of the incorporated MWCNTs at higher current densities. However, at lower current densities, copper electrodeposits only on the deposited copper matrix. In this study, since the current density was 1 A dm^{-2}, which is in the low current density regime, it is considered that copper did not electrodeposit on the protruding ends of the MWCNTs.

Figure 2 shows a cross-sectional SEM image of the Cu/VGCF composite film. The VGCF concentration in the plating bath was 0.5 g dm^{-3}. The black areas in the figure are cross sections of the VGCFs. Thus, the MWCNTs were embedded in the composite films; that is, the tips of the protruding ends of the MWCNTs on the surface of the

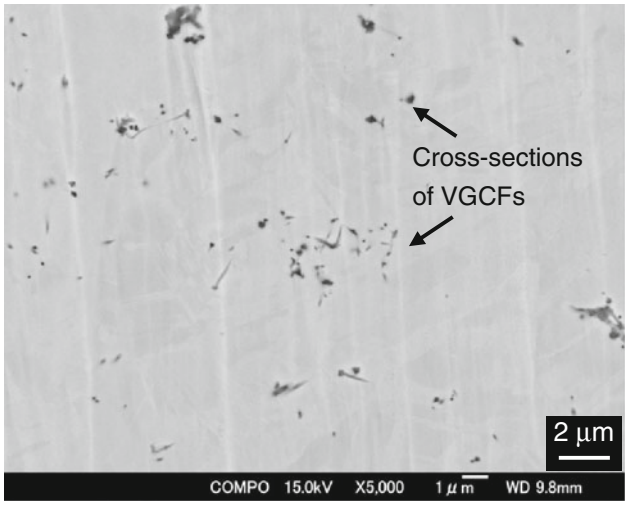

Fig. 2 Cross-sectional SEM image of the Cu/VGCF composite film. The VGCF concentration in the plating bath was 0.5 g dm^{-3}

composite film were fixed by the copper matrix. This structure is considered to be useful to improve the adherence strength of the MWCNTs.

Figure 3 shows the field emission properties of the Cu/MWCNT composite films fabricated from the baths containing various VCGF concentrations. Obvious emission current was measured from each composite film (Fig. 3a). Emission currents were not detected from copper films without the MWCNTs. The emission currents increased with increasing concentration of VGCFs (0.25–0.5 g dm^{-3}) in the plating baths, that is, with increasing number of VGCFs on the composite film surfaces. However, the current density for a VGCF concentration of 2 g dm^{-3} is lower than that of 0.5 g dm^{-3}. Therefore, the aggregation of MWCNTs, shown in Fig. 1b, might be related to the field emission properties.

In general, the field emission current density, J, can be expressed as a function of the external electric field E by Eq. (1) which is referred to as the Fowler–Nordheim equation [29, 30].

$$J = \frac{e^3E^2}{8\pi h\phi t^2(y)}\exp\left[\frac{-8\pi(2m)^{1/2}\phi^{3/2}}{3heE}v(y)\right] \quad (1)$$

where e is the elementary charge, h is Planck's constant, ϕ is the work function of the sample, m is the electron mass, and $t(y)$ and $v(y)$ are the Nordheim elliptic functions.

Transforming Eq. 1, we obtain Eq. 2 as follows,

$$\ln\left(\frac{I}{V^2}\right) = -\frac{b}{V} + \ln a \quad (2)$$

where I is the emission current, V is the voltage, and a and b are constants. Therefore, if the plots of the experimental values of the electron emission current (I) versus applied voltage (V) in the so-called Fowler–Nordheim coordinates,

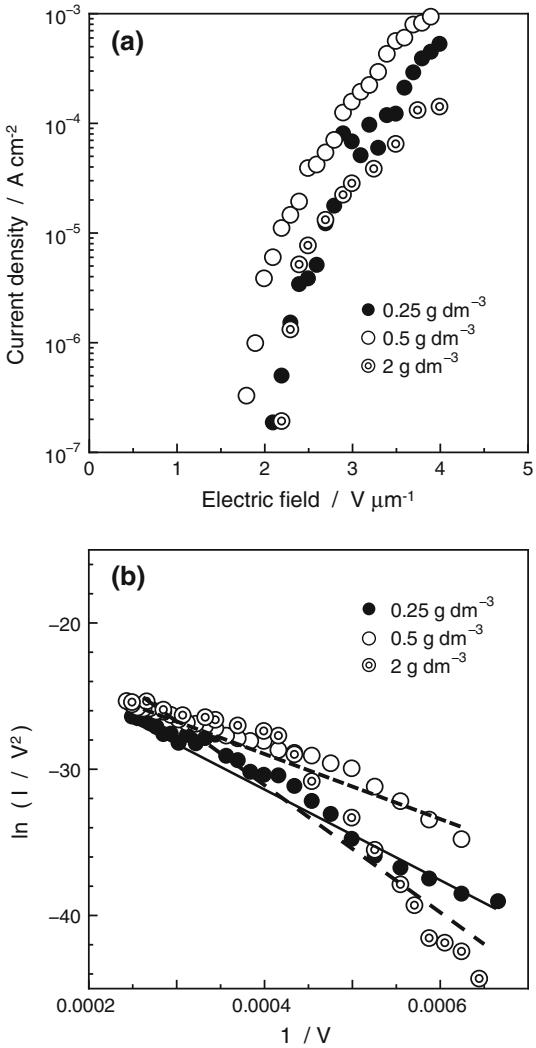

Fig. 3 Relationship between electric field and emission current density of the Cu/VGCF composite films electrodeposited from baths containing various VGCF concentrations (**a**), and the corresponding F–N plots (**b**)

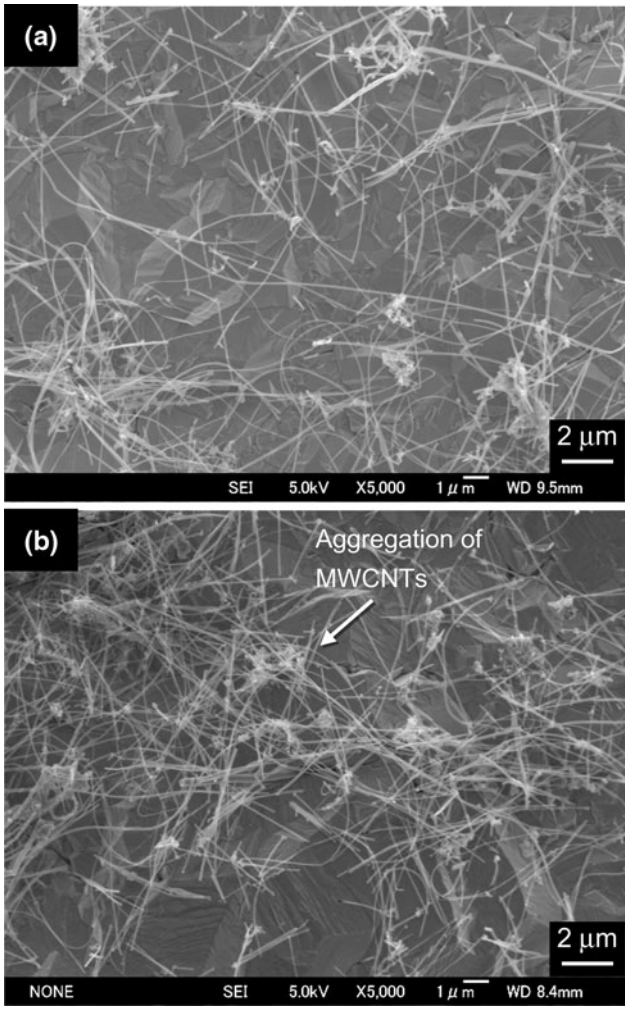

Fig. 4 Surface SEM images of Cu/VGCF-S composite films. The VGCF-S concentration in the plating baths was **a** 0.1 g dm^{-3} and **b** 1 g dm^{-3}

that is, ln (I/V^2) versus $1/V$, are straight lines with negative slopes, the measured emission current of the sample is the field emission current.

Figure 3b shows the corresponding Fowler–Nordheim (F–N) plots. Since these plots are almost straight lines, the measured currents were field emission currents. In other words, the Cu/VGCF composite films are field emitters. The F–N plots, especially for the 2 g dm^{-3} VGCF concentration, are slightly curved. Although the reason for this is not clear, it may be related to the aggregations of VGCFs shown in Fig. 1b.

Figure 4 shows the surface SEM images of the Cu/VGCF-S composite films electrodeposited using plating baths with different VGCF-S concentrations. The VGCF-Ss are present on the surfaces of the composite films. The number of VGCF-Ss increased with increasing VGCF-S concentration (0.1–1 g dm^{-3}) in the plating baths. The orientations of the VGCF-Ss seem to be random. VGCF-Ss are present on the film surface with some aggregation for VGCF-S concentrations ranging from 0.1 to 0.5 g dm^{-3} (Fig. 4a). At a VGCF-S concentration of 1 g dm^{-3}, large aggregates of VGCF-Ss are seen (Fig. 4b). At a VGCF-S concentration >1 g dm^{-3}, the number of VGCF-Ss on the film surface decreased. The VGCF-Ss on the film surfaces were not coated with or deposited with copper, similar to the VGCFs. Furthermore, from cross-sectional observations, the VGCF-Ss were found to be embedded in the composite films, that is, the tips of the protruding ends of the VGCF-Ss on the surface of the composite film were also fixed by the copper matrix.

Figure 5 shows the field emission properties of the Cu/MWCNT-S composite films fabricated from baths containing various VGCF-S concentrations. Again, obvious emission current was measured from each composite film

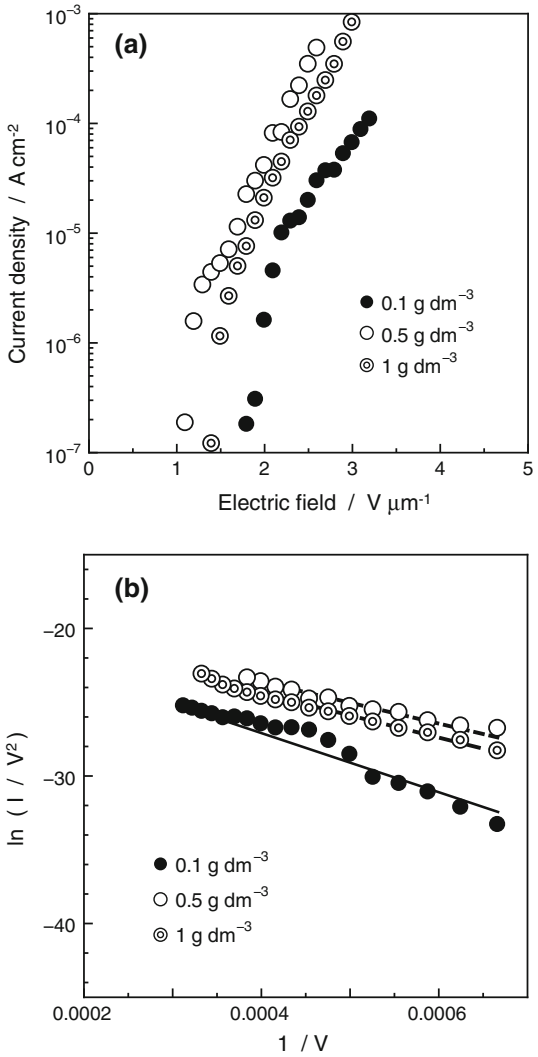

Fig. 5 Relationship between electric field and emission current density of the Cu/VGCF-S composite films electrodeposited from baths containing various VGCF-S concentrations (**a**), and the corresponding F–N plots (**b**)

(Fig. 5a). The emission currents increased with increasing concentration of VGCF-Ss (0.1–0.5 g dm^{-3}) in the plating baths, that is, with increasing number of VGCF-Ss on the composite film surface. However, the current density at a VGCF-S concentration of 1 g dm^{-3} is lower than that at 0.5 g dm^{-3}. Therefore, the aggregation of VGCF-Ss shown in Fig. 4b might be related to the field emission properties. Figure 5b shows the corresponding F–N plots. As described above, since these plots are straight lines, the measured currents are field emission currents, in other words, the Cu/VGCF-S composite films are also field emitters.

Figure 6 shows surface SEM images of Cu/MWNT-7 composite films electrodeposited using plating baths with different MWNT-7 concentrations. The MWNT-7s are present on the surface of the composite films. The number of MWNT-7s slightly increased in the MWNT-7

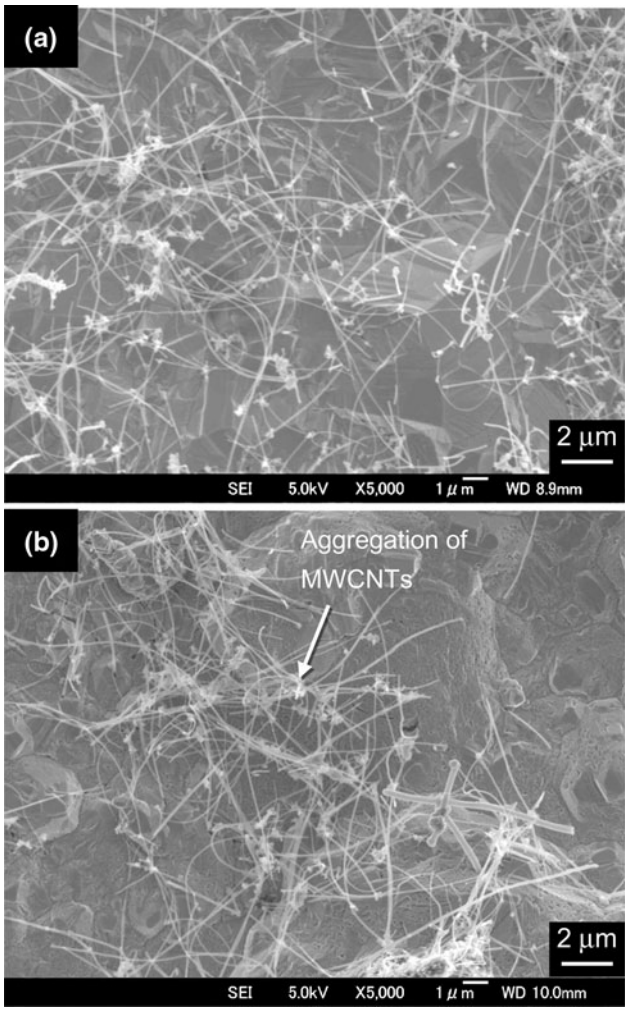

Fig. 6 Surface SEM images of Cu/MWNT-7 composite films. The MWNT-7 concentration in the plating baths was **a** 0.1 g dm^{-3} and **b** 0.75 g dm^{-3}

concentration range of 0.1–0.75 g dm^{-3}. The orientations of the MWNT-7s seemed to be random. The MWNT-7s were present on the film surface with some condensation for MWNT-7 concentrations ranging from 0.1 to 0.25 g dm^{-3} (Fig. 6a). At an MWNT-7 concentration of 0.75 g dm^{-3}, large aggregates of MWNT-7s were seen (Fig. 6b). At an MWNT-7 concentration >0.75 g dm^{-3}, the number of MWNT-7s on the film surface decreased. The MWNT-7s on the film surface were not coated with or deposited by copper, as in the case of VGCFs and VGCF-Ss. Rather, the MWNT-7s were embedded in the composite films. In other words, the tips of the protruding ends of the MWNT-7s on the surface of the composite films were also fixed by the copper matrix.

Figure 7 shows the field emission properties of the Cu/MWNT-7 composite films fabricated from baths containing various MWNT-7 concentrations. Obvious emission current was measured from each composite film

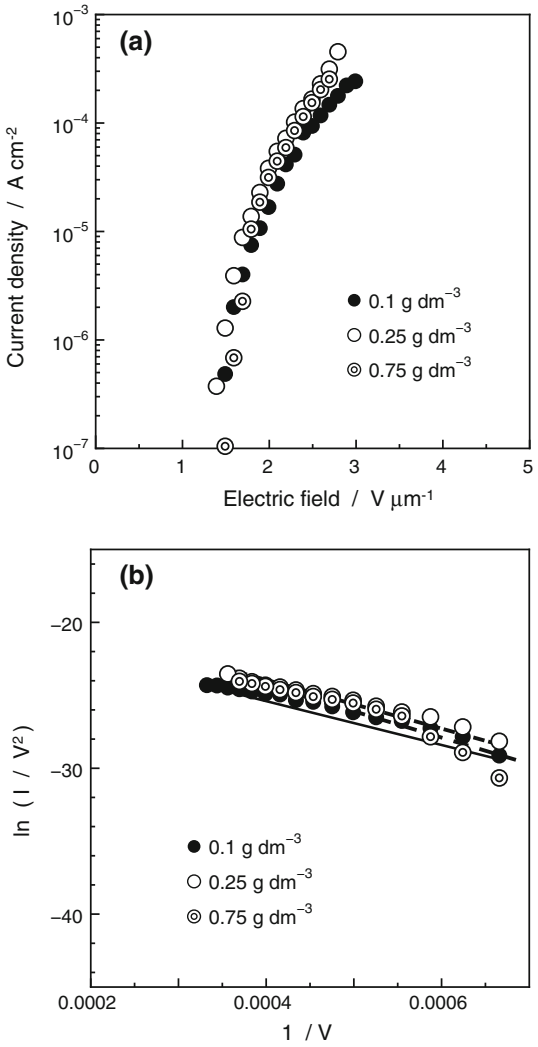

Fig. 7 Relationship between electric field and emission current density of the Cu/MWNT-7 composite films electrodeposited from baths containing various concentrations of MWNT-7 (**a**), and the corresponding F–N plots (**b**)

(Fig. 7a). The emission currents slightly increased for MWNT-7 concentrations ranging from 0.1 to 0.25 g dm^{-3}. However, the current density at a MWNT-7 concentration of 0.75 g dm^{-3} was slightly lower than that at 0.25 g dm^{-3}. Therefore, the aggregation of MWNT-7s shown in Fig. 6b might be related to the field emission properties. Figure 7b shows the corresponding F–N plots. As described above, since these plots are straight lines, the Cu/MWNT-7 composite films are also field emitters.

From Figs. 3, 5, and 7, it is seen that the emission current tended to increase with increasing number of MWCNTs on the composite film surface. This means that the electron emission active sites, mainly the protruding tips of the MWCNTs, increased with increasing number of MWCNTs on the composite film surface. Furthermore, Figs. 3, 5, and 7 show that the formation of aggregations of MWCNTs tended to decrease the emission current in spite of increasing number of MWCNTs on the composite film surface. The tip area of the incorporated MWCNTs might be increased by the aggregation compared to that of independently incorporated MWCNTs, resulting in the lowering of the electric field concentration at the tips and lowering of the emission current.

Table 1 Comparison of turn-on electric fields of the various Cu/MWCNT composite films

Sample	Diameter of MWCNTs (nm)	Turn-on electric field (V μm^{-1})
Cu/VGCF composite film	150	2.1–2.6
Cu/VGCF-S composite film	80	1.6–2.1
Cu/MWNT-7 composite film	60	1.6–1.8

Table 1 shows a comparison of the turn-on electric fields for the various Cu/MWCNT composite films in this study obtained from Figs. 3a, 5a, and 7a. The turn-on electric field is defined as the electric field corresponding to the emission current density of 10 μA cm^{-2}. The turn-on electric fields for the Cu/VGCF composite films, the Cu/VGCF-S composite films, and the Cu/MWNT-7 composite films are in the range of 2.1–2.6, 1.6–2.1, and 1.6–1.8 V μm^{-1}, respectively. Thus, the turn-on electric field appears to be reduced with decreasing diameter of the MWCNTs.

Strictly speaking, it is necessary to quantify the number of MWCNTs on the composite film surface to relate it to the field emission properties. However, accurate quantification of the number of MWCNTs on the composite film surfaces has not yet been achieved. We plan to do this in future work. In any case, the Cu/MWCNT composite films developed here clearly showed field emission properties.

We also investigated the light emission properties of a light emitter that incorporated the Cu/MWCNT composite film field emitter. Figure 8 shows a photograph of the field emission-type light emitter that was manufactured. The Cu/MWNT-7 composite film fabricated from the bath containing 0.25 g dm^{-3} MWNT-7s was used as the field emitter in this case because of its lower turn-on electric field. Light emission from the emitter was clearly observed when a voltage was applied; however, this light emission from the anode area was not uniform. We will investigate the possibility of improving the uniformity of the light emission in future work. Figure 9 shows the variation of the brightness of the field emission-type light emitter with time. The cathode-gate voltage and cathode–anode voltage were 2.3 and 4.0 kV, respectively. A brightness level of around 100 cd m^{-2} continued for about 100 h. The fluctuation of the light emission was somewhat significant. In the present study, since the light emission stability test was stopped at 96 h, it is considered that stable light emission should

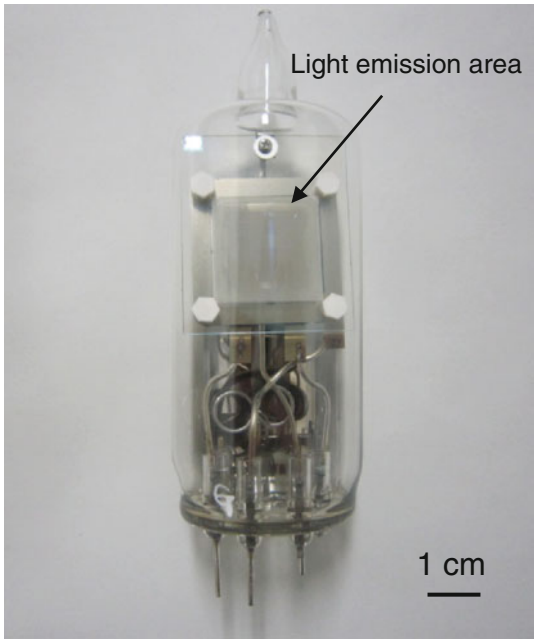

Fig. 8 A field emission-type light emitter

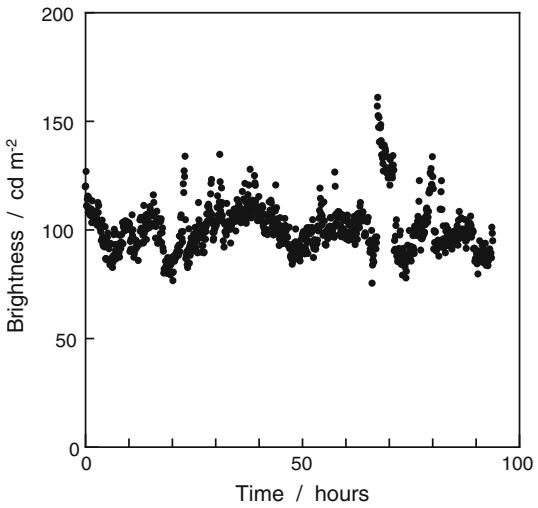

Fig. 9 Variation of brightness of the field emission-type light emitter as a function of time. The field emitter used was the Cu/MWNT-7 composite film. The cathode-gate voltage and the cathode–anode voltage were 2.3 and 4.0 kV, respectively

continue for more than 100 h. Thus, the stability of light emission can be qualitatively stated to be reasonably good.

4 Conclusions

Cu/MWCNT composite films with various MWCNT diameters were successfully fabricated by an electrodeposition technique. Bare MWCNTs were present on the composite film surfaces, and the tips of the protruding ends of the MWCNTs were fixed by the copper matrix. The Cu/MWCNT composite films showed field emission properties, and their turn-on electric field tended to decrease with decreasing diameter of the MWCNTs. A triode-type white light-emitting device incorporating the Cu/MWCNT composite film as the cathode emitted white light of around 100 cd cm^{-2} for approximately 100 h. Metal/CNT composite films fabricated by electrodeposition can thus be expected to be used as field emission cathodes for practical applications.

Acknowledgments This research was supported by a Grant-in-Aid for Scientific Research (C) and the Regional Innovation Cluster Program of Nagano, granted by MEXT, Japan.

References

1. Oberlin A, Endo M, Koyama T (1976) J Cryst Growth 32:335
2. Iijima S, Ichihashi T (1993) Nature 363:603
3. Kuzumaki T, Ujiie O, Ichinose H, Ito K (2000) Adv Eng Mater 2:416
4. He CN, Zhao NQ, Shi CS, Song SZ (2009) J Alloys Compd 487:258
5. Wenzhong T, Michael HS, Suresh GA (2003) Carbon 412:779
6. Chen W, Tao X, Xue P, Cheng X (2005) Appl Surf Sci 252:1404
7. Xiong J, Zheng Z, Qin X, Li M, Li H, Wang X (2006) Carbon 44:2701
8. Arai S, Endo M, Sato T, Koide A (2006) Electrochem Solid-State Lett 9:C131
9. Cai D, Song M (2008) Carbon 462:107
10. Rinzler AG, Hafner JH, Nikolaev P, Lou L, Kim SG, Tomanek D, Nordlander P, Colbert DT, Smalley RE (1995) Science 269:1550
11. de Heer WA, Chatelain A, Ugarte D (1995) Science 270:1179
12. Sohn JI, Lee S (2001) Appl Phys Lett 78:901
13. Huh Y, Lee JY, Lee CJ (2005) Thin Solid Films 475:267
14. Siegal MP, Miller PA, Provencio PP, Tallant DR (2007) Diam Relat Mater 161:793
15. Choi WB, Chung DS, Kang JH, Kim HY, Jin YW, Han IT, Lee YH, Jung JE, Lee NS, Park GS, Kim JM (1999) Appl Phys Lett 75:3129
16. Zhao WJ, Sawada A, Takai M (2002) Jpn J Appl Phys 41:4314
17. Li J, Lei W, Zhang X, Zhou X, Wang Q, Zhang Y, Wang B (2003) Appl Surf Sci 220:96
18. Lee HJ, Lee YD, Moon SI, Cho WS, Lee YH, Kim JK, Hwang SW, Ju BK (2006) Carbon 44:2625
19. Cheng CW, Chen CM, Lee TC (2009) Appl Surf Sci 255:5770
20. Lee YD, Lee KS, Lee YH, Ju BK (2007) Appl Surf Sci 254:513
21. Fan YC, Liu YM, Chen YC, Sung T, Ger MD (2009) Appl Surf Sci 255:7753
22. Huang BR, Lin TC, Yang YK, Tzeng SD (2010) Diam Relat Mater 19:158
23. Arai S, Saito T, Endo M (2008) Electrochem Solid-State Lett 11:D72
24. Arai S, Saito T, Endo M (2010) J Electrochem Soc 157:D127
25. Endo M, Kim YA, Hayashi T, Nishimura K, Matusita T, Miyashita K, Dresselhaus MS (2001) Carbon 39:1287
26. Arai S, Endo M (2003) Electrochem Commun 5:797
27. Arai S, Endo M, Kaneko N (2004) Carbon 42:641
28. Arai S, Saito T, Endo M (2010) J Electrochem Soc 157:D147
29. Fowler RH, Nordheim DL (1928) Roy Soc Proc A119:173
30. Temple D (1999) Mater Sci Eng R24:185